

## Adenovirus-mediated interleukin-18 mutant *in vivo* gene transfer inhibits tumor growth through the induction of T cell immunity and activation of natural killer cell cytotoxicity

Kyung-Sun Hwang,<sup>1</sup> Won-Kyung Cho,<sup>1</sup> Jinsang Yoo,<sup>1</sup> Young Rim Seong,<sup>2</sup> Bum-Kyeng Kim,<sup>3</sup> Samyong Kim,<sup>4</sup> and Dong-Soo Im<sup>1</sup>

<sup>1</sup>Cell Biology Laboratory/Gene Therapy Research Unit, Korea Research Institute of Bioscience and Biotechnology, Yusong, Daejeon, Republic of Korea; <sup>2</sup>Samyang Genex Biotech Research Institute, Daejeon, Republic of Korea; <sup>3</sup>Department of Pathology, College of Medicine, Konyang University, Daejeon, Republic of Korea; and <sup>4</sup>Department of Internal Medicine, College of Medicine, Chungnam National University, Daejeon, Republic of Korea.

We report here that gene transfer using recombinant adenoviruses encoding interleukin (IL)-18 mutants induces potent antitumor activity *in vivo*. The precursor form of IL-18 (ProIL-18) is processed by caspase-1 to produce bioactive IL-18, but its cleavage by caspase-3 (CPP32) produces an inactive form. To prepare IL-18 molecules with an effective antitumor activity, a murine IL-18 mutant with the signal sequence of murine granulocyte-macrophage (GM)-colony stimulating factor (CSF) at the 5'-end of mature IL-18 cDNA (GMmIL-18) and human IL-18 mutant with the prepro leader sequence of trypsin (PPT), which is not cleaved by caspase-3 (PPTHIL-18CPP32<sup>-</sup>), respectively, were constructed. Adenovirus vectors carrying GMmIL-18 or PPTHIL-18CPP32<sup>-</sup> produced bioactive IL-18. Ad.GMmIL-18 had a more potent antitumor effect than Ad.mProIL-18 encoding immature IL-18 in renal cell adenocarcinoma (Renca) tumor-bearing mice. Tumor-specific cytotoxic T lymphocytes, the induction of Th1 cytokines, and an augmented natural killer (NK) cell activity were detected in Renca tumor-bearing mice treated with Ad.GMmIL-18. An immunohistological analysis revealed that CD4<sup>+</sup> and CD8<sup>+</sup> T cells abundantly infiltrated into tumors of mice treated with Ad.GMmIL-18. Huh-7 human hepatoma tumor growth in nude mice with a defect of T cell function was significantly inhibited by Ad.PPTHIL-18CPP32<sup>-</sup> compared with Ad.hProIL-18 encoding immature IL-18. Nude mice treated with Ad.PPTHIL-18CPP32<sup>-</sup> contained NK cells with increased cytotoxicity. The results suggest that the release of mature IL-18 in tumors is required for achieving an antitumor effect including tumor-specific cellular immunity and augmented NK cell-mediated cytotoxicity. These optimally designed IL-18 mutants could be useful for improving the antitumor effectiveness of wild-type IL-18.

Cancer Gene Therapy (2004) 11, 397–407. doi:10.1038/sj.cgt.7700711

Published online 26 March 2004

**Keywords:** IL-18 mutant; adenovirus vector; renal cancer; liver cancer

Cancer immunogene therapy has been a challenging but promising modality among the various gene therapeutic approaches, since it may have great potential for abrogating malignant tumor cells under microenvironment by generating tumor-specific immune responses in the host. Interleukin (IL)-18, previously known as interferon (IFN)- $\gamma$  inducing factor,<sup>1</sup> augments the cytotoxicity of T and natural killer (NK) cells, and the proliferation of T cells, and stimulates Th (helper) 1 cells to produce IL-2 and IFN- $\gamma$ .<sup>2,3</sup> The biological activities of IL-18 suggest that it has potential for the treatment of cancer by inducing tumor-specific cellular immunity as

well as activating NK cells in the host. In fact, a number of studies have revealed that the recombinant IL-18 protein contains antitumor activity against various types of murine tumor cell lines *in vivo*.<sup>3,4</sup>

IL-18 is produced in the form of a biologically inactive precursor (ProIL-18) by cells in the immune system as well as by nonimmune cells.<sup>5–8</sup> ProIL-18 does not contain a known signal peptide-sequence, and is converted into the bioactive, mature form by proteolytic cleavage by the action of caspase-1.<sup>9,10</sup> It has recently been shown that ProIL-18 is cleaved by proteinase-3 at different site(s) from that of caspase-1 and that the cleavage product retains IFN- $\gamma$ -inducing activity.<sup>11</sup> ProIL-18 or mature IL-18 is also cleaved by caspase-3 (CPP32) and the cleavage inactivates the immunological function of IL-18.<sup>12</sup> In order to increase the antitumor effectiveness of IL-18 gene transfer, it would be desirable to design a bioactive IL-18 mutant that can be efficiently secreted from cells and/or

Received April 10, 2003.

Address correspondence and reprint requests to: Dr Dong-Soo Im, Cell Biology Laboratory/Gene Therapy Research Unit, Korea Research Institute of Bioscience and Biotechnology, Yusong, Daejeon 305-333, Republic of Korea. E-mail: tmdongsu@kribb.re.kr

resistant to the inactivation by caspase-3. It has been shown that a recombinant adenoviral vector carrying the prepro leader sequence of human parathyroid hormone linked to the 5' end of the mature murine IL-18 cDNA (Ad.PTH-IL-18) completely eradicated murine MCA205 tumor in mice mainly by enhancing the activity of NK cells, but not T cell immunity.<sup>13</sup> Colon cancer cells transfected with the plasmid vector containing mature IL-18 cDNA with the Igk leader sequence were found to function as a tumor vaccine mainly through T cell activation, but not NK cell activation.<sup>14</sup> Human pancreatic carcinoma cells transduced with a retroviral vector expressing IL-18 gene did not exhibit any antitumor effect in nude mice that were devoid of T cells.<sup>15</sup>

Adenovirus vectors have been used extensively in cancer gene therapy, because they deliver therapeutic genes into cells or tissues efficiently and the transduced genes are expressed transiently and strongly.<sup>16</sup> We constructed recombinant adenoviruses that express and release bioactive, mature mIL-18 and caspase-3-resistant, mature hIL-18 mutants, respectively. We evaluated the antitumor effectiveness of adenoviral vectors carrying the mutated IL-18 genes in renal cell adenocarcinoma (Renca)-bearing mice and Huh-7 human hepatoma-bearing nude mice, and immune cells that are involved in the antitumor effect of IL-18. We found that the mature mIL-18 mutant exhibits a more potent antitumor activity than the immature mIL-18 *in vivo*, induces tumor-specific cellular immunity, and enhances NK cell activity as well. The recombinant adenovirus expressing the mature hIL-18 mutant also exhibited a modest, but significant antitumor effect in a mouse tumor model with a defect in T cell function.

## Materials and methods

### Cells and cell culture

Renca, YAC-1, Huh-7, HeLa, 293, or RAW cells were maintained in RPMI-1640 (Gibco-BRL), high- or low-glucose Dulbecco's modified Eagle medium (DMEM), or Iscove's modified Dulbecco's medium, which were supplemented with 10% fetal bovine serum (FBS) and penicillin/streptomycin in an atmosphere of 5% CO<sub>2</sub> chamber at 37°C.

### Cloning of IL-18 and construction of IL-18 mutants

The murine ProIL-18 cDNA was amplified by reverse transcriptase-polymerase chain reaction (RT-PCR) of total RNA extracted from RAW cells with the primers (5'-GATAAGCTTACCATGGCTGCCATGTCAGAAG-3' and 5'-CTCGAATTCACCTTTGATGTAAGTTAGTG-3') and tagged with the Flag epitope at its C-terminus. To generate GMmIL-18, the signal sequence of GM-CSF (17 amino acids) was polymerase chain reaction (PCR)-amplified and linked to the amino-terminus of mature, murine IL-18. Human ProIL-18 cDNA was cloned by PCR-amplification of human liver cDNA library with the primers (5'-CTCGAATTCACCATG-

GCTGCTGAACCAAG-3' and 5'-TTCCTGCAGCTAG-TCTTCGTTTTGAAC-3'). Human ProIL-18CPP32<sup>-</sup> mutant, which is resistant to the cleavage by caspase-3, was generated by site-directed mutagenesis using two-step PCR. To introduce mutations at the caspase-3 recognition sites, the first PCR was performed with an internal sense primer encoding glutamic acid instead of aspartic acid at amino acids 71 and 76 of human ProIL-18 (5'-AGATATGACTGAGTCTGACTGTAGAGAGAATGC-3') and an antisense primer encoding Flag epitope after the open reading frame of hProIL-18 (5'-TTCCTGCA-GGCTCTTCGTTTTGAACAGT-3'). The second PCR was performed using the amplified PCR product (379 bp) as a reverse primer and a sense primer (5'-CTCGAATTCACCATGGCTGCTGAACCAAG-3'). To generate mature hIL-18CPP32<sup>-</sup> with the preprotrypsin (PPT) signal sequence, mature hIL-18CPP32<sup>-</sup> DNA was PCR-amplified from human ProIL-18CPP32<sup>-</sup> by using primers (5'-CATAAGCTTTACTTTGGCAAGCTA-GAATC-3' containing *Hind*III site and 5'-CGTGGATC-CCTAGTCTTCGTTTTGAAC-3' containing *Bam*HI site) and cloned into the *Hind*III-*Bam*HI site of pFlagCMV1 containing PPT signal sequence and Flag epitope at its amino-terminus (Invitrogen). The cloned mProIL-18, GMmIL-18, hProIL-18, and hIL-18CPP32<sup>-</sup> cDNAs were confirmed by sequencing, and inserted into pX.dCMV.pA, an adenovirus shuttle plasmid harboring CMV promoter, multiple cloning sites, and poly(A) sequences, by a standard cloning procedure.

### Preparation of recombinant adenoviruses

293 cells were cotransfected with adenoviral backbone plasmid pBHG10 or pJM17 and the shuttle plasmids pX.dCMV.pA encoding IL-18 variants by a standard calcium phosphate method. Recombinant adenoviruses were purified by a single plaque isolation. Correct recombinant adenoviruses were confirmed by restriction enzyme analyses of viral DNAs. Recombinant adenoviruses for animal studies were propagated in 293 cells, and purified by sequential centrifugation in CsCl step gradient as previously reported.<sup>17</sup> Virus titers were determined on 293 cells as plaque forming unit (PFU).

### Immunoblotting and immunoprecipitation

HeLa cells were plated on 60-mm dishes at a density of  $5 \times 10^5$  cells. Cells were transduced with recombinant adenoviruses at a multiplicity of infection (MOI) of 100 in serum-free DMEM for 2 hours. Mock- or virus-transduced cells were harvested in RIPA buffer (10 mM Tris-HCl (pH 8.2), 150 mM NaCl, 1% NP-40, 1% sodium deoxycholate, and 0.1% SDS) at 48 hours postinfection. The culture media were saved to detect secreted IL-18. Cleared cell extracts were prepared by centrifugation following sonic treatment. Cleared cell extracts (50 µg) were subjected to SDS-15% PAGE. Proteins on the gels were transferred to PVDF membranes. The membranes were blocked with 10% skim milk in phosphate-buffered saline (PBS) including 0.05% tween 20 and incubated with mouse anti-Flag antibody as primary antibody, and

goat anti-mouse antibody conjugated with horseradish peroxidase as a secondary antibody. Proteins were detected according to Amersham's ECL protocol. Culture supernatants were incubated with anti-Flag antibody-conjugated agarose beads for 4 hours at 4°C. Proteins bound to the beads were washed three times with wash-buffer (40 mM N-2-hydroxyethylpiperazine-N'-2-ethane sulfonic acid (pH 7.4), 100 mM KCl, 0.1% NP-40, 0.1 mM DTT) and once with PBS, and subjected to immunoblotting using mouse anti-Flag antibody, as described above.

#### Establishment and treatment of mice tumors

Female BALB/c mice, 7–8 weeks of age, were purchased from the animal breeding laboratory in the Korea Research Institute of Bioscience and Biotechnology, adjusted to five mice per cage, and kept in isolation under strictly controlled specific-pathogen-free conditions. Animals were exposed to 12-hours light/12-hours dark cycles, and standard feed and water were provided *ad libitum*. Tumors were generated by the subcutaneous injection of  $1.5 \times 10^5$  cells of Renca or  $1.5 \times 10^6$  cells of Huh-7 in 0.1 ml of PBS on the flank of BALB/c or BALB/c-nude mice. After visible tumors had developed at 8–9 days after tumor cell-inoculation, the mice were injected intratumorally once with  $1 \times 10^9$  PFU of recombinant adenoviruses in 50  $\mu$ l of injection buffer (10 mM Tris-HCl (pH 7.4), 1 mM MgCl<sub>2</sub>, 10% glycerol). Tumor sizes were measured prior to virus injection and subsequently at 3-day intervals or twice a week. Linear calipers were used to measure the longest diameter a and width b. The tumor size was calculated using the formula:  $(a \times b^2/2)$ .

#### Cytotoxicity assays

The cytolytic activity of cytotoxic T lymphocytes (CTL) or NK cells was determined by standard 4-hours <sup>51</sup>Cr-release assays. Mice spleens were removed aseptically 21 days after virus treatment. Unicellular suspensions were prepared by passing the spleens through a metal mesh. Red blood cells were lysed by suspending the splenocytes in 2 ml of a lysis buffer for red blood cells (Sigma). The splenocytes were then used as effector cells for NK cell activity assay. Renca cells were treated with mitomycin C at 50  $\mu$ g/ml for 20 min at 37°C. The splenocytes were cocultured with the inactivated Renca cells for 5 days in the presence of recombinant human IL-2 (2 ng/ml) (Sigma), and then used as effector cells in a cytotoxicity assay of CTL. Renca or YAC-1 cells ( $2 \times 10^6$ ) in 0.5 ml of RPMI-1640 with 20% FBS were labeled with 50  $\mu$ Ci of Na<sup>51</sup>CrO<sub>4</sub> (Amersham) for 90 minutes. The labeled cells were washed three times with serum-free DMEM and used as target cells. Target cells ( $1 \times 10^4$  cells/well) were then mixed with effector cells in a U-bottomed 96-well plate for 4 hours at 37°C at three effector-to-target ratios (100:1, 33:1, and 11:1) in triplicate. The mixtures of target and effector cells were incubated for 4 hours at 37°C. The percentage of specific <sup>51</sup>Cr release was calculated as [(cpm experimental release – cpm spontaneous release/cpm maximum release – cpm spontaneous release)]  $\times$  100.

The maximum <sup>51</sup>Cr release was determined from the supernatant of the labeled cells lysed by the addition of 0.1 ml of 3% SDS. The extent of spontaneous release was determined from the supernatant of the labeled cells incubated in 0.1 ml of medium without effector cells. The standard deviation of each sample in triplicate and for spontaneous release was less than 10 and 20%, respectively.

#### Enzyme-linked immuno sorbent assays for IFN- $\gamma$ and IL-2

Basically, enzyme-linked immuno sorbent assays (ELISAs) were performed with reagents and procedures described in the product literature supplied by Endogen (USA). Flat-bottomed 96-well microtiter plates (Nunc Maxisorp) were used for ELISAs. The ELISA plates were coated with rat anti-IL-2 or anti-IFN- $\gamma$  antibodies (10  $\mu$ g/ml) at 4°C overnight and blocked with 4% bovine serum albumin in PBS for 2 hours at 37°C. The splenocytes ( $2 \times 10^6$  cells/ml) from the tumor-bearing mice 21 days after virus treatment were stimulated with the inactivated Renca cells in U-bottomed 96-well plates, as described above, at an effector-to-stimulator ratio of 10:1. Supernatants (50  $\mu$ l) from 24, 48, or 72 hours cultures were added to the wells of the ELISA plates, followed by incubation for 1 hour. After several wash steps, rat anti-IL-2 or anti-IFN- $\gamma$  antibodies conjugated with biotin were added. Color was developed using avidin-conjugated horseradish peroxidase and OPD substrate (Sigma). The reaction was terminated by the addition of 2 N H<sub>2</sub>SO<sub>4</sub>. Absorbance was measured at 490 nm with an ELISA plate reader. The amounts of IL-2 or IFN- $\gamma$  were quantified by interpolation of a standard curve generated using known amounts of standard recombinant IL-2 or mouse IFN- $\gamma$  (Endogen). The biological activity of murine or human IL-18 produced from the recombinant adenoviruses was assessed based on their ability to induce IFN- $\gamma$  secretion from murine splenocytes or human peripheral blood mononuclear cells (hPBMCs). The hPBMCs were obtained from blood from healthy human volunteers by Ficoll-Hypaque density centrifugation. The hPBMCs or murine splenocytes ( $1.5 \times 10^6$  cells/well) were washed with cold medium, and incubated with culture supernatants that contained IL-18. IFN- $\gamma$  in supernatants from 24 hours cultures was determined using ELISA, as described above.

#### Immunohistochemistry

Tumors were excised from the mice on day 21 after the injection of recombinant adenoviruses, immediately frozen, and embedded in OCT compound at –70°C. Serial 7-mm sections were prepared from the tumors using a cryostat, and subjected to immunochemical staining using anti-mouse CD4 and CD8 $\alpha$  antibodies (Pharmin-gen) with a LASB kit (DAKO). Sections were visualized by the reaction of streptavidin-alkaline phosphatase with AEC as the chromogen.

## Statistics

Statistical analysis was carried out using the unipolar, paired Student's *t*-test and the two-sided  $\chi^2$  test. The antitumor effects were considered statistically significant when the *P*-value was less than .05.

## Results

### Cells transduced with recombinant adenoviruses encoding IL-18 mutants produce bioactive IL-18 proteins

Since ProIL-18 lacks a signal peptide and the extracellular release of the mature IL-18 is considered to be important for its effective antitumor effect, the signal peptide of granulocyte-macrophage colony stimulating factor (GM-CSF) was linked to the 5'-end of the mature mL-18 cDNA. Since ProIL-18 or mature IL-18 can be inactivated by CPP32, which possibly results in a low level of production of bioactive IL-18, a mature hIL-18 mutant was constructed with two point mutations at the cleavage sites of CPP32, in which the PPT signal sequence is linked to its amino-terminus. The hIL-18CPP32<sup>-</sup> protein was not cleaved by caspase-3 *in vitro* (data not shown). We constructed recombinant adenoviruses carrying these IL-18 mutants, Ad.GmIL-18 and Ad.PPTHIL-18CPP32<sup>-</sup>, Ad.mProIL-18 encoding immature mL-18, and Ad.hProIL-18 encoding immature hIL-18 (Fig 1). The ProIL-18 and IL-18 mutants were tagged with Flag-epitope at their N- or C-termini to permit their detection.

We examined whether cells transduced with the recombinant adenoviruses produce mature and bioactive IL-18. HeLa cells were transduced with the recombinant adenoviruses encoding immature or mature IL-18, or GFP as a control at an MOI of 100. Equivalent amounts of culture supernatants were immunoprecipitated with anti-Flag antibody. Equivalent amounts of cell extracts and the immunoprecipitates were analyzed by immunoblotting with anti-Flag antibody. Immature IL-18 with a size of 24 kDa and mature IL-18 with a size of 18 kDa were detected in the protein extracts and culture supernatants of the cells transduced with the relevant recombinant adenoviruses (Fig 2a and b). To examine whether IL-18 proteins present in the culture media were bioactive, splenocytes of naïve mice or hPBMCs were treated with equivalent amounts of the culture media of the cells transduced with Ad.mIL-18 or Ad.hIL-18 viruses. The IFN- $\gamma$  contents in the incubation mixtures were measured using ELISA. Splenocytes treated with the culture supernatant from Ad.GMmIL-18 virus-transduced cells produced a significantly higher level of IFN- $\gamma$  than those of Ad.mProIL-18 or controls, indicating that Ad.GMmIL-18 expresses bioactive IL-18 (Fig 2c,  $P < .021$  for Ad.mProIL-18 *versus* Ad.GMmIL-18,  $P < .0009$  for Mock *versus* Ad.GMmIL-18). The hPBMCs treated with the culture supernatant of Ad.PPThIL-18CPP32<sup>-</sup> virus-transduced cells also produced a significantly higher level of IFN- $\gamma$  than those of Ad.hProIL-18 or the controls,

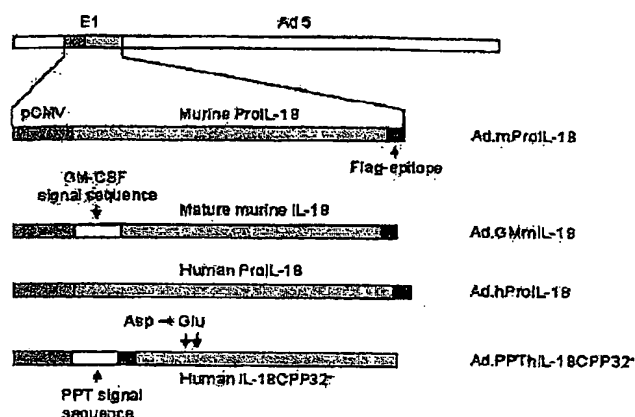


**Figure 1** Schematic illustration of recombinant adenoviruses encoding the wild type and mutants IL-18. IL-18 cDNAs, inserted into the deleted E1 region of adenovirus type 5 genome, are under the transcriptional control of the immediate-early gene promoter of human cytomegalovirus (pCMV). Black rectangles indicate the location of Flag-epitope. Ad.mProIL-18 encodes immature, murine IL-18. Ad.GMmIL-18 encodes mature mIL-18 with the signal sequence of GM-CSF at its N-terminus. Ad.hProIL-18 encodes immature, hIL-18. Ad.PPTnIL-18CPP32<sup>32</sup> encodes immature hIL-18 with the prepro leader sequence of trypsin (PPT), in which aspartic acids at amino acid positions 71 and 76 were substituted with glutamic acids. Asp<sup>71</sup>-Ser<sup>72</sup> and Asp<sup>76</sup>-Asn<sup>77</sup> are the cleavage sites by CPP32 (caspase-3).<sup>12</sup>

indicating that the hIL-18 mutant with the two point mutations retains its biological activity (Fig 2d,  $P < .0154$  for Ad.hProIL-18 *versus* Ad.PPThIL-18CPP32<sup>-</sup>,  $P < .0073$  for Mock *versus* Ad.PPThIL-18CPP32<sup>-</sup>). The culture supernatants containing the immature IL-18 appeared to have a slightly higher IFN- $\gamma$ -producing ability than controls, although the activity differences between the two groups were not significant (Fig 2c and d,  $P < .07$  for Mock *versus* Ad.mProIL-18,  $P < .11$  for Mock *versus* Ad.hProIL-18). This may account for a modest antitumor activity of adenoviral vectors carrying immature IL-18 compared to Ad.GFP (Fig 3a and 6a). The IFN- $\gamma$ -producing activity of the culture supernatant of Ad.PPThIL-18CPP32<sup>-</sup> was one order of magnitude less than that of Ad.GMmIL-18. Presumably, this may result from the different assay conditions used, namely the use of mouse splenocytes for mIL-18 and hPBMCs for hIL-18.

*Ad.GMmIL-18. has a more potent antitumor activity than Ad.mProlL-18*

We compared the antitumor effect of Ad.GMmIL-18 with Ad.mProIL-18 at equal PFU in Renca -tumor-bearing mice. Tumor growth was inhibited more strongly by treatment with Ad.GMmIL-18 than with Ad.mProIL-18 by day 12 (Fig 3a). We investigated the relative antitumor

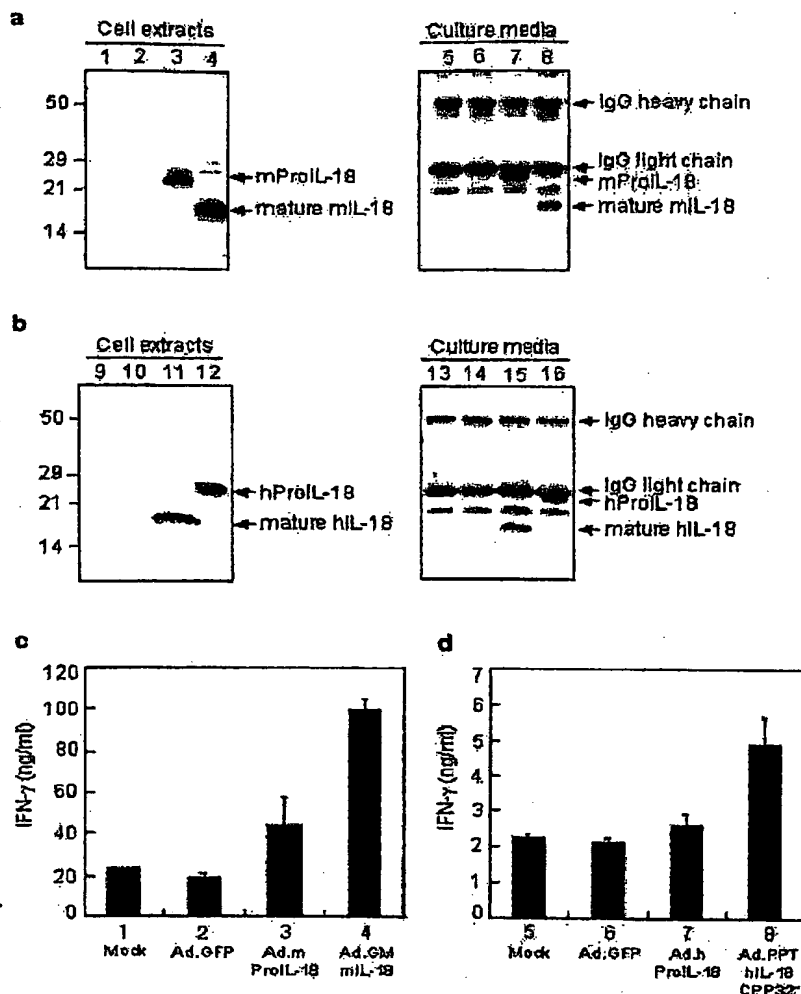


**Figure 2** Adenoviral vectors carrying IL-18 mutants produce bioactive IL-18 proteins. (a) HeLa cells were transduced without (lanes 1 and 5) or with Ad.GFP (lanes 2 and 6), Ad.mProIL-18 (lanes 3 and 7), or Ad.GMmIL-18 (lanes 4 and 8) at an MOI of 100. Culture supernatants (lanes 5–8) were immunoprecipitated with anti-Flag antibody. Cell extracts (lanes 1–4) and the immunoprecipitates were analyzed by immunoblotting with anti-Flag antibody. Molecular size markers are shown at the left in kilodaltons (kDa). Arrows indicate the positions of immature and mature mIL-18 protein and the heavy and light chain of immunoglobulin G (IgG). (b) HeLa cells were transduced without (lanes 9 and 13) or with Ad.GFP (lanes 10 and 14), Ad.hProIL-18 (lanes 11 and 15), or Ad.PPTHIL-18CPP32- (lanes 12 and 16) at an MOI of 100. The presence of hIL-18 proteins in cell extracts (lanes 9–12) and culture supernatants (lanes 13–16) was determined as described above. (c, d) HeLa cells were transduced without or with the indicated recombinant adenoviruses at an MOI of 100. Cells were harvested with culture media at 48 hours post-transduction. Culture supernatants were obtained by centrifugation. Murine splenocytes (lanes 1–4) or hPBMCs (lanes 5–8) were incubated with 100 µl of the culture supernatants of cells transduced without or with the indicated recombinant adenoviruses for 24 hours. Recombinant IL-12 (20 ng/ml) was present in the incubation mixtures with hPBMCs. The amounts of interferon-γ in the supernatants of the incubation mixtures were measured using ELISA. Data are the mean ± SD of three independent experiments in duplicate.

effectiveness of Ad.GMmIL-18 compared with Ad-mProIL-18 by survival analysis. Three out of eight mice treated with Ad.GMmIL-18 survived more than 60 days, while only one of the eight mice treated with Ad-mProIL-18 survived to 60 days. Median survivals of the

mice treated with Ad-mProIL-18 and with Ad.GMmIL-18 were 32.8 and 41.1 days, respectively. Thus, Ad.GMmIL-18 treatment resulted in a significant survival benefit compared to Ad-mProIL-18 treatment ( $P < .021$ ).

**Ad.GMmIL-18 treatment induces tumor-specific cytotoxic T lymphocytes, production of Th1 cytokines, and enhances cytotoxicity of NK cells in Renca tumor-bearing mice**

Since Ad.GMmIL-18 exerted a stronger antitumor effect than Ad.mProIL-18 in Renca tumor-bearing mice, we focused on Ad.GMmIL-18 to examine which immune cells are involved in the antitumor activity of mIL-18. We initially compared the antitumor activity of Ad.GMmIL-18 with that of Ad.GFP using a large number of experimental animals. Tumor growth inhibition in Renca tumor-bearing mice treated with Ad.GMmIL-18 or Ad.GFP is shown in Figure 3c and the treatment outcome is summarized in Table 1. The Ad.GMmIL-18 treatment

inhibited tumor growth more strongly than Ad.GFP. Four of 20 mice treated with Ad.GMmIL-18 became tumor-free and a delay of tumor growth was observed in eight of 20 mice. The antitumor effect of Ad.GMmIL-18 was statistically significant in comparison with that of Ad.GFP ( $P < .0098$ ). The antitumor effect was also significant ( $P < .035$ ), even when mice with complete tumor regression were counted.

We next examined whether Ad.GMmIL-18 treatment induced tumor-specific cytotoxic T lymphocytes. Effector cells were prepared from the splenocytes of tumor-bearing mice treated with Ad.GMmIL-18 or Ad.GFP. Renca cells labeled with  $^{51}\text{Cr}$  were used as target cells. A 4-hours chromium release assay was carried out. Although the specific lysis of target cells was low, the effector cells from the mice treated with Ad.GMmIL-18 lysed Renca cells three-fold more effectively than those treated with Ad.GFP (Fig 4a). We next examined whether Ad.GMmIL-18 treatment induced Th1 cytokines. Splenocytes from tumor-bearing mice treated with Ad.GMmIL-18 or Ad.GFP were incubated with inactivated Renca cells. The IL-2 and IFN- $\gamma$  content in the supernatants of the incubation mixtures were measured using ELISA 24, 48, or 72 hours after incubation, respectively (Fig 4c and d). IL-2 was increased more than two-fold in the splenocytes of mice treated with Ad.GMmIL-18 in comparison with Ad.GFP at 48 hours. IFN- $\gamma$  was also increased more than two-fold in the splenocytes of mice treated with Ad.GMmIL-18 compared with Ad.GFP by 72 hours. We next examined whether Ad.GMmIL-18 treatment increased the activity of NK cells. The splenocytes of tumor-bearing mice treated with Ad.GMmIL-18 or Ad.GFP were used as effector cells. YAC-1 cells were labeled with  $^{51}\text{Cr}$ , and used as target cells. The specific lysis of target cells by the effector cells was determined by a  $^{51}\text{Cr}$  release assay. The effector cells from

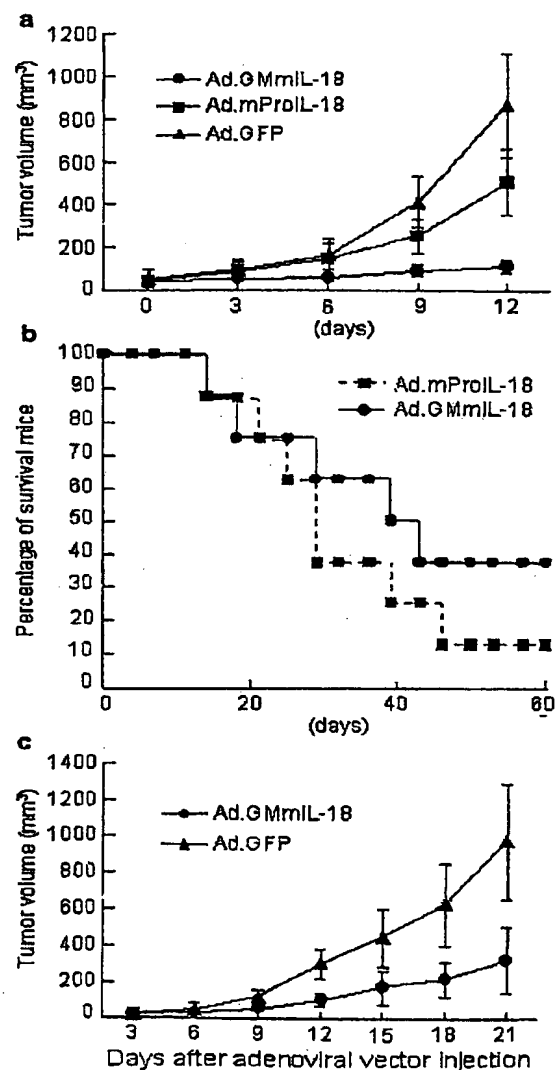


**Figure 3** Ad.GMmIL-18 shows a more potent antitumor effect than Ad.mProIL-18 or Ad.GFP in the Renca tumor-bearing mice. (a) Renca tumors were established by the subcutaneous inoculation of mice with  $1.5 \times 10^5$  cells of Renca. The experimental animals in which tumors reached a diameter of 4–5 mm were randomly divided into three treatment groups ( $n=5$  per group) and intratumorally administered once with  $1 \times 10^9$  PFU of Ad.GMmIL-18, Ad.mProIL-18, or Ad.GFP on day 0. Tumor growth was measured at 3-day intervals. The mean values of tumor sizes in each group are indicated. Bar represents mean  $\pm$  SD. (b) Long-term survival analysis. The Renca tumor-bearing mice were established, and divided into two groups ( $n=8$  per group). Mice in each group were intratumorally injected once with Ad.GMmIL-18 or Ad.mProIL-18 viruses as described above. One mouse became tumor-free and two mice experienced a significant delay of tumor growth in the Ad.GMmIL-18 treatment group and three of eight mice survived for 60 days. One out of eight mice with Ad.mProIL-18 treatment became tumor-free and survived for 60 days. (c) The Renca tumor-bearing mice were grouped by two ( $n=20$  per group). The mice in each group were intratumorally injected once with Ad.GMmIL-18 or Ad.GFP as described above for day 0. Graphic representations of the mean tumor growth for day 3 through 21 are shown. Bar represents mean  $\pm$  SD. Treatment outcome is summarized in Table 1.

**Table 1** Tumor regression following intratumoral injection of Ad.GMmIL-18 or Ad.GFP

Treatment	N	P-value <sup>a</sup>	P-value <sup>b</sup>	Response		
				Complete	Partial	No response
Ad.GMmIL-18	20	0.0098	0.035	4	8	8
Ad.GFP	20			0	4	16

N means number of Renca tumor-bearing mice intratumorally injected once with Ad.GMmIL-18 or Ad.GFP at  $1 \times 10^9$  PFU.

<sup>a</sup>P-value states statistical significance of complete plus partial antitumor effects of Ad.GMmIL-18 compared with Ad.GFP.

<sup>b</sup>P-value states statistical significance of only the complete response of Ad.GMmIL-18 compared with Ad.GFP.

Complete refers to animals that have undergone total and permanent regression of the established tumor for 21 days after viral injection. Partial refers to animals that have undergone partial tumor regression followed by regrowth, or a significant delay in growth. No response refers to animals whose tumors have continued to grow at a rate comparable to controls.

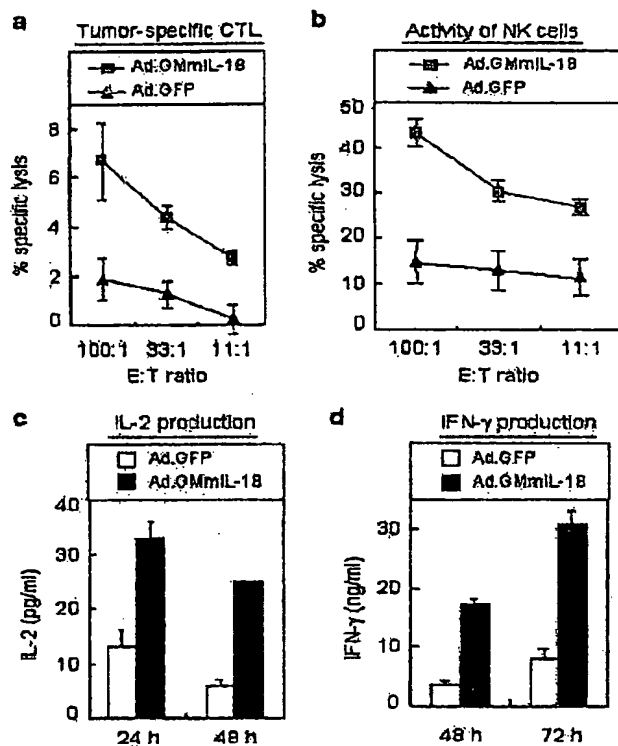


**Figure 4** Ad.GMmIL-18 treatment induces tumor-specific CTL, Th1 cytokines, and enhances the cytotoxicity of NK cells in Renca tumor-bearing mice. The mice splenocytes ( $n=3$  per group) were isolated from the treatment groups described in Figure 3c on day 21 after adenoviral injection and used as effector cells in a  $^{51}\text{Cr}$  release assay. Both Renca and YAC-1 cells labeled with  $^{51}\text{Cr}$  were used as target cells for CTL assay (a) and NK cells assay (b), respectively. The percentage of specific lysis was determined. (c, d) Mice splenocytes ( $n=3$  per group) were isolated from the treatment groups as described in Figure 3c on day 21 after adenoviral injection, and incubated with inactivated Renca cells. Culture supernatants of the incubated cells were obtained at the indicated times. Amounts of IL-2 (c) and IFN- $\gamma$  (d) in the supernatants were measured using ELISA. Bar represents mean  $\pm$  SD.

mice treated with Ad.GMmIL-18 lysed target cells about three-fold more effectively in comparison with those with Ad.GFP at a 100:1 effector-to-target cell ratio (Fig 4b).

#### Histology of mice tumor treated with Ad.GMmIL-18

We examined the distribution of CD4<sup>+</sup> and CD8<sup>+</sup> T cells immunohistologically in tumors of mice treated with Ad.GMmIL-18 or Ad.GFP. A number of lymphocytes infiltrated into the tumor in mice treated with Ad.GMmIL-18, while relatively small numbers of lymphocytes were detected mainly at the periphery of the tumor in mice treated with Ad.GFP (Fig 5a, b versus c, d). When CD8<sup>+</sup> and CD4<sup>+</sup> T cells were counted in three different fields of tissues at  $\times 200$  magnification, the mean cell numbers of CD8<sup>+</sup> and CD4<sup>+</sup> T were significantly higher in tumor tissues treated with Ad.GMmIL-18 than in those with Ad.GFP ( $32.3 \pm 4.5$  versus  $11.7 \pm 3.5$  for CD8<sup>+</sup> T cell numbers of Ad.GMmIL-18 versus Ad.GFP,  $P < .001$ , and  $37.7 \pm 3.5$  versus  $18.0 \pm 2.7$  for CD4<sup>+</sup> T cell numbers of Ad.GMmIL-18 versus Ad.GFP,  $P < .001$ ).

#### Ad.PPThIL-18CPP32<sup>-</sup> treatment exhibits an antitumor activity and enhances cytotoxicity of NK cells in Huh-7 tumor-bearing nude mice

To examine whether the gene transfer of the human IL-18 mutant exhibits antitumor activity in the mice tumor model with a defect in T cell function, we established a BALB/c nude mice tumor model by the transplantation of Huh-7 human hepatoma cells. Tumor growth inhibition in the tumor-bearing mice treated with Ad.PPThIL-18CPP32<sup>-</sup>, Ad.hProIL-18, or Ad.GFP is shown in Figure 6a. The mean tumor growth of mice treated with Ad.PPThIL-18CPP32<sup>-</sup> was significantly inhibited in comparison with mice treated with Ad.hProIL-18 or Ad.GFP ( $P < .006$  and  $P < .009$ , respectively). We next examined whether NK cell activity was augmented in mice treated with Ad.PPThIL-18CPP32<sup>-</sup> compared to Ad.hProIL-18 or Ad.GFP. The splenocytes of tumor-bearing mice treated with the recombinant adenoviruses were prepared and used as effector cells. A  $^{51}\text{Cr}$  release assay was carried out with YAC-1 cells as target cells. The splenocytes of mice treated with Ad.PPThIL-18CPP32<sup>-</sup>

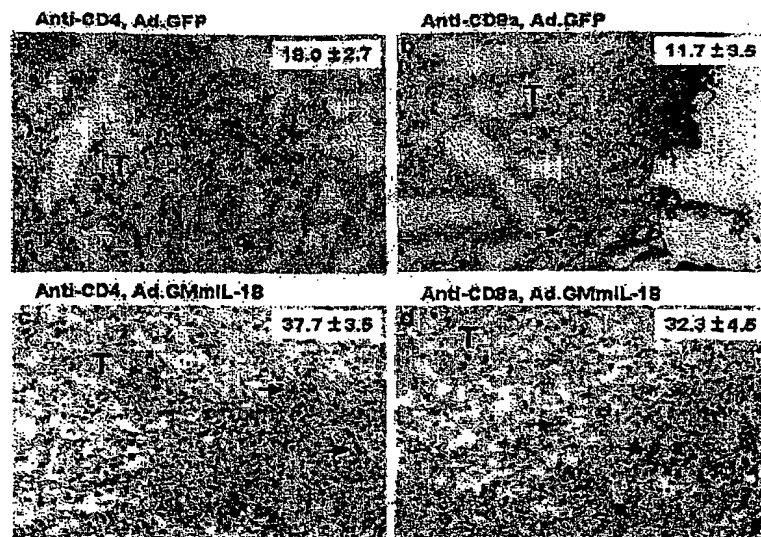


**Figure 5** Immunohistochemical analysis of CD8a<sup>+</sup> and CD4<sup>+</sup> T cells present in tumors of Renca tumor-bearing mice treated with Ad.GMmIL-18 or Ad.GFP. Tumor tissues were obtained on day 21 from the Renca tumor-bearing mice treated with Ad.GMmIL-18 (c, d) or Ad.GFP (a, b) and analyzed as described in Materials and methods. Histological analysis was performed with two animals in each group. The numbers of CD4<sup>+</sup> and CD8a<sup>+</sup> T lymphocytes were counted in three different fields of tumor samples of mice treated with Ad.GMmIL-18 or Ad.GFP at  $\times 200$  magnification, and averaged. Representative photographs ( $\times 200$ ) with the mean numbers of the immuno-stained cells are shown. Arrows indicate T lymphocytes stained with anti-CD4 (a, c) and anti-CD8a (b, d) antibodies. T; tumor cells.

contained a higher cytolytic activity of NK cells than those treated with Ad.hProIL-18 or Ad.GFP (Fig 6b).

## Discussion

The activation of the host immune system in cancer patients may increase the therapeutic potential by inducing a systemic and tumor-specific cellular immunity even at a low level of therapeutic gene delivery *in vivo*.<sup>18</sup> This notion encouraged us to investigate whether IL-18 gene transfer using an adenovirus vector exerts an antitumor effect in mice tumor models and which immune cells are involved in tumor eradication or regression. Although the involvement of caspase-1 was proposed in the processing/secretion of ProIL-18, the mechanism of secretion of mature IL-18 has not been clearly established at the molecular level.<sup>9,10,19-22</sup> To construct mature IL-18 mutants the processing/secretion of which are independent on caspase-1, we linked the signal sequence of GM-CSF or preprotypsin to the 5'-end of mature IL-18 cDNAs, because we previously observed that a recombinant adenovirus encoding mGM-CSF efficiently secreted mGM-CSF into the culture media,<sup>23</sup> and the PPT leader sequence has frequently been used for the secretion of proteins. Indeed, Ad.GMmIL-18 and Ad.PPThIL-18CPP32<sup>-</sup> secreted mature IL-18 proteins outside the cells (Fig 2). Unexpectedly, we found that immature IL-18 proteins were present in the culture media of cells

transduced with adenoviral vectors encoding precursor IL-18 (Fig 2a and b). Since the cytopathic effect of the adenovirus vectors at 100 MOI was found to be negligible, this finding suggests that the immature IL-18 could be released outside the cell by an unknown mechanism. This result is consistent with the presence of precursor IL-18 in the culture supernatant of PBMCs.<sup>20</sup> Culture supernatants containing the mature IL-18 proteins resulted in higher levels of IFN- $\gamma$  production compared with those containing precursor IL-18 (Fig 2c and d, lanes 3 and 7 versus 4 and 8). Presumably, this accounts for the more potent antitumor activity of Ad.GMmIL-18 and Ad.PPThIL-18CPP32<sup>-</sup> than Ad-mProIL-18 and Ad.hProIL-18 in the tumor-bearing mice, respectively (Figs 3 and 6). Thus, our results indicate that the release of the mature IL-18 is required for achieving increased antitumor activity. The importance of the mature IL-18 secretion for the antitumor activity of IL-18 was recently demonstrated in murine CT-26, Renca, and B16F10 melanoma tumor models.<sup>13,14,24-26</sup> Among various mature IL-18 secretion vectors with different signal sequences, it appeared to be impossible to examine which one is optimal for the efficient secretion of mature IL-18, because mature IL-18 secretion vectors were constructed in different manners and their biological activities were also determined under different conditions using different cells.

Viral infection enhances the gene expression of caspase-1 and caspase-3 in human macrophages, and induces the cleavage of procaspases into their mature forms.<sup>27</sup>



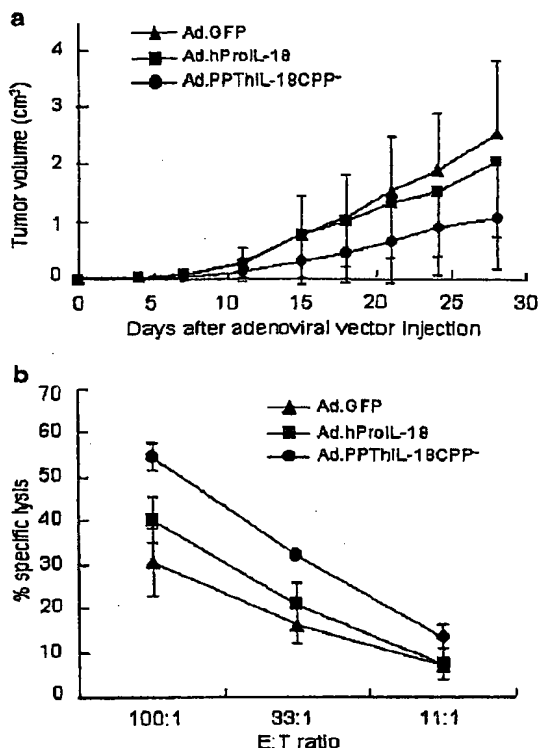


**Figure 6** Ad.PPThIL-18CPP32<sup>-</sup> exhibits a more potent antitumor activity than Ad.hProIL-18 or Ad.GFP and increases the cytolytic activity of NK cells. (a) Huh-7 tumors were established in BALB/c nude mice by the subcutaneous inoculation of  $1.5 \times 10^6$  cells. The experimental animals in which tumors reached a diameter of 4–5 mm were randomly divided into three treatment groups ( $n=6$  per group). Mice were intratumorally administered once with  $1 \times 10^8$  PFU of Ad.PPThIL-18CPP32<sup>-</sup>, Ad.hProIL-18, or Ad.GFP on day 0. Tumor growth was measured twice per week. Graphic representations of the mean tumor growth overtime are shown. The bar represents the mean  $\pm$  SD. (b) Splenocytes of the Huh-7 tumor-bearing mice were isolated from the treatment groups ( $n=3$  for each group) on day 21 after virus administration and were used as effector cells in a  $^{51}\text{Cr}$  release assay. YAC-1 cells labeled with  $^{51}\text{Cr}$  were used as target cells. The percentage specific lysis was determined as described in Materials and methods. The bar represents the mean  $\pm$  SD.

Although this situation does not reflect perfectly tumor cells infected with Ad.IL-18 virus, caspase-1 and caspase-3 might be expressed and activated in some tumor cells after treatment with the adenovirus vector. The activation of caspase-1 in tumor cells treated with Ad.ProIL-18 viruses might have resulted in the release of mature IL-18. This possibility may account for the modest antitumor effects of Ad.mPro-IL18 and Ad.hProIL-18 compared to Ad.GFP (Figs 3a and 6a). The activation of caspase-3 would result in a low level of production of mature IL-18 and consequently decrease the antitumor activity of Ad.IL-18. To further investigate this possibility, we

attempted initially, but were not successful in constructing a caspase-3-resistant and secretive mIL-18 mutant, although it is not known whether mIL-18 is cleaved by caspase-3 and where the cleavage site is located in mIL-18. Therefore, we constructed the Ad.PPThIL18CPP32<sup>-</sup> virus and investigated its antitumor activity. We were not able to determine whether the caspase-3-resistant, mature hIL-18 mutant is more potent than mature hIL-18 in terms of antitumor effectiveness because of the lack of a control virus, Ad.PPThIL-18. Nevertheless, we show here that Ad.PPThIL18CPP32<sup>-</sup> released the mature and bioactive hIL-18 (Fig 2d) and exhibited a stronger antitumor activity than Ad.hProIL-18 (Fig 6a). Thus, our results indicate at least that an IL-18 molecule with more potent antitumor activity than the immature IL-18 can be designed. In particular, the other limiting factor that inhibits or decreases the antitumor activity of IL-18, except for its secretion, might be the IL-18 binding protein (IL-18BP).<sup>28</sup> IL-18BP is present in a 20-fold molar excess compared to IL-18, circulating constitutively in healthy subjects, and can neutralize the function of IL-18.<sup>29</sup> IL-18BP is expressed constitutively in some tumor cells.<sup>29</sup> It has been shown that the mature IL-18 mutant with E42A and K89A mutations exhibited four-fold greater IFN- $\gamma$ -inducing activity and was not neutralized by IL-18BP compared with the wild-type IL-18.<sup>30</sup> It will be interesting to examine the issue of whether the IL-18 mutant with a defect in the binding to IL-18BP will exhibit more potent antitumor activity than the wild type or other IL-18 mutants.

We were able to detect tumor-specific CTL in Renca tumor-bearing mice treated with Ad.GMmIL-18 (Fig 4a). The increased production of Th1 cytokines such as IL-2 and IFN- $\gamma$  was detected in the splenocytes of mice treated with Ad.GMmIL-18 (Fig 4c and d). An immunohistological analysis revealed that CD4<sup>+</sup> and CD8<sup>+</sup> T cells had abundantly infiltrated into the tumors of mice treated with Ad.GMmIL-18 compared to Ad.GFP (Fig 5). However, the infiltration of NK cells in the tumor sections from mice treated with Ad.GMmIL-18 or Ad.GFP was not detected (data not shown). These results suggest that T cell-mediated immunity might have been generated more or less in mice treated with Ad.GMmIL-18. The result of the immunohistological analysis (Fig 5) is different from the previous result, in which a marked reduction in the number of CD8<sup>+</sup> cells within the tumor was detected by the treatment of MCA205 tumor-bearing mice with Ad.PTH.IL-18, and a sparse penetration of CD4<sup>+</sup> cells was observed within the tumor regardless of treatment.<sup>13</sup> This might have resulted from different tumor models treated with adenoviral vectors carrying IL-18 constructed differently. Immunostaining of tumor samples excised from MCA205 tumor-bearing mice was performed on day 2 following Ad.PTH.IL-18 treatment, while immunostaining of the tumor samples excised from the Renca tumor-bearing mice was performed on day 21 after Ad.GMmIL-18 treatment. Therefore, we think that the difference likely results from tumor samples that were collected at different times. A sparse infiltration of CD4<sup>+</sup> T cells and a dense infiltration of CD8<sup>+</sup> T cells in the

tumor were observed 14 days after the subcutaneous injection of CT 26 tumor cells constitutively expressing the mature IL-18.<sup>14</sup> CD8<sup>+</sup> and CD4<sup>+</sup> T cells have been shown to play key roles in the antitumor immunity of the combined gene transfer of IL-18 with cytosine deaminase.<sup>31</sup> Thus, the results suggest that T cell-mediated immunity, including CD8<sup>+</sup> T cells, is involved in the antitumor activity of IL-18.

Both the enhanced cytotoxicity of NK cells and the induction of tumor-specific CTL were detected in Renca tumor-bearing mice treated with Ad.GMmIL-18 (Fig 4). The Ad.PPThIL18CPP32<sup>-</sup> treatment significantly inhibited tumor growth in Huh-7 tumor-bearing mice and increased the cytotoxicity of NK cells (Fig 6). However, no significant survival benefit was observed in Huh-7 tumor-bearing nude mice treated with Ad-PPThIL18CPP32<sup>-</sup> compared with Ad.hProIL-18, while a significant survival benefit was found in Renca tumor-bearing mice treated with Ad.GMmIL-18 compared with Ad.mProIL-18 (Fig 3b). Presumably, this might result from the fact that hIL-18 may not function as well as mIL-18 in mice. Alternatively, the results suggest that the enhancement of NK cell activity or other pathway(s) for tumor regression is not sufficient for exerting a potent antitumor activity of the mature hIL-18 in the host, or that T cell immune response is indispensable.

The *in vitro* IFN- $\gamma$  production abilities of Ad.IL-18 viruses appear to correlate with their antitumor effects *in vivo*. The IFN- $\gamma$  produced in response to IL-12 has been shown to inhibit angiogenesis by inducing the IFN-inducible protein 10.<sup>32</sup> The antiangiogenic activity of IL-18 appeared to be specifically mediated by IFN- $\gamma$ .<sup>33</sup> It has also been suggested that the antiangiogenic pathway of IL-18 may not be completely mediated through IFN- $\gamma$  signaling.<sup>34</sup> Therefore, IFN- $\gamma$  produced in response to IL-18 gene transfer or another antiangiogenic pathway could have inhibited tumor growth via the inhibition of angiogenesis. The NK cell cytotoxicity of endothelial cells, however, has been proposed as a potential mechanism by which IL-12 can suppress neovascularization.<sup>35</sup> Thus, the increased cytotoxicity of NK cells appears to play an important role in tumor regression by IL-18 gene transfer (Figs 4b and 6b), although we cannot exclude the possibility that the antitumor effect of IL-18 mutants might have resulted from the inhibition of angiogenesis by IFN- $\gamma$  or other mechanisms. It has been suggested that IL-18 enhances NK cell activity, inducing the death of viable tumor cells that in turn is acquired and processed by dendritic cells to promote CTL generation from naïve T cells.<sup>36-38</sup> Our findings that IL-18 gene transfer enhanced NK cell cytotoxicity in Huh-7 tumor-bearing nude mice and induced tumor-specific CTL in Renca tumor-bearing mice, which resulted in significant tumor growth inhibitions, are in favor of the hypothesis that tumor cell destruction by NK cells is an important initiating event in the induction of tumor-specific CTL by IL-18 gene transfer.<sup>36</sup>

In conclusion, we demonstrated here that the gene transfer of designed IL-18 mutants exhibited potent antitumor activity in Renca and Huh-7 hepatoma animal

models, and the induction of tumor-specific cellular immunity and augmentation of NK cell activity were involved in the antitumor effectiveness of IL-18. The relative and precise roles of T cell immunity, NK cells, or other pathway(s) in the antitumor activity of IL-18 remain to be determined in detail. Nevertheless, our results suggest that IL-18 mutants with an increased antitumor activity can be designed and could be useful in cancer gene therapy, and can serve as useful tools in the studies of biological roles of IL-18.

## Acknowledgments

We thank Sanghyeon Kim for cloning of IL-18 cDNAs, and JS Lim and KD Kim for immunological assays. This work was supported by a Grant (FG03-32-02) of 21C Frontier Functional Genome Project from the Ministry of Science and Technology, South Korea. Kyung-Sun Hwang and Won-Kyung Cho have contributed equally to this work.

## References

1. Okamura H, Tsutsi H, Komatsu T, et al. A novel cytokine that induces IFN- $\gamma$  production by T cells. *Nature*. 1995;378:88-91.
2. Dinarello CA, Novick D, Puren AJ, et al. Overview of interleukin-18: more than an interferon- $\gamma$  inducing factor. *J Leuk Biol*. 1998;63:658-664.
3. Nakanishi K, Yoshimoto T, Tsutsui H, Okamura H. Interleukin-18 regulates both Th1 and Th2 responses. *Annu Rev Immunol*. 2001;19:423-474.
4. Golab J. Interleukin 18 — interferon  $\gamma$  inducing factor — a novel player in tumor immunotherapy? *Cytokine*. 2000;12:332-338.
5. Stoll S, Muller G, Kurimoto M, et al. Production of IL-18 (IFN- $\gamma$ -inducing factor) messenger RNA and functional protein by murine keratinocytes. *J Immunol*. 1997;159:298-302.
6. Udagawa N, Horwood NJ, Elliott J, et al. Interleukin-18 (interferon- $\gamma$ -inducing factor) is produced by osteoblasts and acts *via* granulocyte/macrophage-stimulating factor and not *via* interferon- $\gamma$  to inhibit osteoclast formation. *J Exp Med*. 1997;185:1005-1012.
7. Conti B, Jahng JW, Tinti C, et al. Induction of interferon- $\gamma$  inducing factor in the adrenal cortex. *J Biol Chem*. 1997;272:2035-2037.
8. Cho D, Song H, Kim YM, et al. Endogenous interleukin-18 modulates immune escape of murine melanoma cells by regulating the expression of Fas ligand and reactive oxygen intermediates. *Cancer Res*. 2000;60:2703-2709.
9. Ghayur T, Banerjee S, Hugunin M, et al. Caspase-1 processes IFN- $\gamma$ -inducing factor and regulates LPS-induced IFN- $\gamma$  production. *Nature*. 1997;386:619-623.
10. Gu Y, Kuida K, Tsutsui H, et al. Activation of interferon- $\gamma$  inducing factor mediated by interleukin-1 $\beta$  converting enzyme. *Science*. 1997;275:206-209.
11. Fantuzzi G, Dinarello CA. Interleukin-18 and interleukin-1 beta: two cytokines substrates for ICE (caspase-1). *J Clin Immunol*. 1999;19:1-11.

12. Akita K, Ohtsuki T, Nukada Y, et al. Involvement of caspase-1 and caspase-3 in the production and processing of mature human interleukin 18 in monocytic THP.1 cells. *Biol Chem.* 1997;272:26595-26603.
13. Osaki T, Hashimoto W, Gambotto A, et al. Potent antitumor effects mediated by local expression of the mature form of the interferon- $\gamma$  inducing factor, interleukin-18 (IL-18). *Gene Ther.* 1999;6:808-815.
14. Yoshimura K, Hazama S, Iizuka N, et al. Successful immunogene therapy using colon cancer cells (colon 26) transfected with plasmid vector containing mature interleukin-18 cDNA and the Ig $\kappa$  leader sequence. *Cancer Gene Ther.* 2001;8:9-16.
15. Yoshida Y, Tasaki K, Kimurai M, et al. Antitumor effect of human pancreatic cancer cells transduced with cytokine genes which activate Th1 helper T cells. *Anticancer Res.* 1998;18:333-335.
16. Weitzman MD, Wilson JM, Eck SL. Adenovirus vectors in cancer gene therapy. In: Sobol RE and Scanlon KJ, eds. *The Internet Book of Gene Therapy, Cancer Therapeutics*. CJ, USA: Appleton & Lange; 1995: 17-25.
17. Seong YR, Choi S, Lim JS, et al. Immunogenicity of the E1E2 proteins of hepatitis C virus expressed by recombinant adenoviruses. *Vaccine.* 2001;19:2955-2964.
18. Vile RG, Russell SJ, Lemoine NR. Cancer gene therapy: hard lessons and new courses. *Gene Ther.* 2000;7: 2-9.
19. Oshikawa K, Shi F, Rakhmilevich AL, et al. Synergistic inhibition of tumor growth in a murine mammary adenocarcinoma model by combinational gene therapy using IL-12, pro-IL-18, and IL-1 $\beta$  converting enzyme cDNA. *Proc Natl Acad Sci USA.* 1999;96:13351-13356.
20. Puren AJ, Fantuzzi G, Dinarello CA. Gene expression, synthesis, and secretion of interleukin 18 and interleukin 1 $\beta$  are differentially regulated in human blood mononuclear cells and mouse spleen cells. *Proc Natl Acad Sci USA.* 1999;96:2256-2261.
21. Perregaux D, McNiff P, Laliberte R, Conklyn M, Gabel CA. ATP acts as an agonist to promote stimulus-induced secretion of IL-1 $\beta$  and IL-18 in human blood. *J Immunol.* 2000;165:4615-4623.
22. Mehta VB, Hart J, Wewers MD. ATP-dependent release of interleukin (IL)-1 $\beta$  and IL-18 requires priming by lipopolysaccharide and is independent of caspase-1 cleavage. *J Biol Chem.* 2001;276:3820-3826.
23. Sanghyeon Kim, Suh KS, Seong YR, et al. Adenovirus-mediated mGM-CSF *in vivo* gene transfer inhibits tumor growth in a murine Meth A fibrosarcoma model. *J Kor Soc Virol.* 2000;30:141-150.
24. Hara S, Nagai H, Miyake H, et al. Secreted type of modified interleukin-18 gene transduction into mouse renal cell carcinoma cells induces systemic tumor immunity. *J Urol.* 2001;165:2039-2043.
25. Goto H, Osaki T, Nishino K, et al. Construction and analysis of new vector systems with improved interleukin-18 secretion in a xenogeneic human tumor model. *J Immunother.* 2002;25:S35-S41.
26. Nagai H, Hara I, Horikawa T, et al. Gene transfer of secreted-type modified interleukin-18 gene to B16F10 melanoma cells suppresses *in vivo* tumor growth through inhibition of tumor vessel formation. *J Invest Dermatol.* 2002;119:541-548.
27. Pirhonen J, Sareneva T, Julkunen I, Matikainen S. Virus infection induces proteolytic processing of IL-18 in human macrophages via caspase-1 and caspase-3 activation. *Eur J Immunol.* 2001;31:726-733.
28. Novick D, Kim SH, Fantuzzi G, et al. Interleukin-18 binding protein: a novel modulator of the Th1 cytokine response. *Immunity.* 1999;10:127-136.
29. Kim SH, Eisenstein M, Reznikov L, et al. Structural requirements of six naturally occurring isoform of the IL-18 binding protein to inhibit IL-18. *Proc Natl Acad Sci USA.* 2000;97:1190-1195.
30. Kim SH, Azam T, Yoon DY, et al. Site-specific mutations in the mature form of human IL-18 with enhanced biological activity and decreased neutralization by IL-18 binding protein. *Proc Natl Acad Sci USA.* 2001;98:3304-3309.
31. Ju DW, Yang Y, Tao Q, et al. Interleukin-18 gene transfer increases antitumor effects of suicide gene therapy through efficient induction of antitumor immunity. *Gene Therapy.* 2000;7:1672-1679.
32. Sgadari C, Angiolillo AL, Tosato G. Inhibition of angiogenesis by interleukin-12 is mediated by the interferon-inducible protein-10. *Blood.* 1996;87:3877-3882.
33. Coughlin CM, Salhany KE, Wysocka M, et al. Interleukin-12 and interleukin-18 synergistically induces murine tumor regression which involves inhibition of angiogenesis. *J Clin Invest.* 1998;101:1441-1452.
34. Cao R, Farnebo J, Kurimoto M, Cao Y. Interleukin-18 acts as an angiogenesis and tumor suppressor. *FASEB J.* 1999;13:2195-2202.
35. Yao L, Sgadari C, Furuke K, et al. Contribution of natural killer cells to inhibition of angiogenesis by interleukin-12. *Blood.* 1999;93:1612-1621.
36. Micallef MJ, Tanimoto T, Kohno K, Ikeda M, Kurimoto M. Interleukin 18 induces the sequential activation of natural killer cells and cytotoxic T lymphocytes to protect syngeneic mice from transplantation with Meth A sarcoma. *Cancer Res.* 1997;57:4557-4563.
37. Tanaka F, Hashimoto W, Okamura H, et al. Rapid generation of potent and tumor-specific cytotoxic T lymphocytes by interleukin-18 using dendritic cells and natural killer cells. *Cancer Res.* 2000;60:4838-4844.
38. Ju DW, Tao Q, Lou G, et al. Interleukin 18 transfection enhances antitumor immunity induced by dendritic cell-tumor cell conjugates. *Cancer Res.* 2001;61:3735-3740.

**This Page is Inserted by IFW Indexing and Scanning  
Operations and is not part of the Official Record**

**BEST AVAILABLE IMAGES**

Defective images within this document are accurate representations of the original documents submitted by the applicant.

Defects in the images include but are not limited to the items checked:

- ☐ **BLACK BORDERS**
- ☐ **IMAGE CUT OFF AT TOP, BOTTOM OR SIDES**
- ☐ **FADED TEXT OR DRAWING**
- ☐ **BLURRED OR ILLEGIBLE TEXT OR DRAWING**
- ☐ **SKEWED/SLANTED IMAGES**
- ☐ **COLOR OR BLACK AND WHITE PHOTOGRAPHS**
- ☐ **GRAY SCALE DOCUMENTS**
- ☐ **LINES OR MARKS ON ORIGINAL DOCUMENT**
- ☐ **REFERENCE(S) OR EXHIBIT(S) SUBMITTED ARE POOR QUALITY**
- ☐ **OTHER:** \_\_\_\_\_

**IMAGES ARE BEST AVAILABLE COPY.**

**As rescanning these documents will not correct the image problems checked, please do not report these problems to the IFW Image Problem Mailbox.**